

COLLIMATION STRATEGY FOR THE LOW-EMITTANCE PETRA IV STORAGE RING

M. A. Jebramcik*, I. Agapov, S. A. Antipov, R. Bartolini, R. Brinkmann, D. Einfeld, T. Hellert, J. Keil, Deutsches Elektronen-Synchrotron (DESY), 22607 Hamburg, Germany

Abstract

The beam-intensity losses in the proposed PETRA IV electron storage ring that will replace DESY's synchrotron light source PETRA III will be dominated by the Touschek effect due to the high bunch density. The beam lifetime will only be in the range of 5 h in the timing mode (80 high-intensity bunches) leading to a maximum power loss of 170 mW along the storage ring (excluding injection losses). To avoid the demagnetization of the permanent-magnet undulators and combined-function magnets, this radiation-sensitive hardware has to be shielded against losses as well as possible. Such shielding elongates the lifetime of the hardware and consequently reduces the time and the resources that are spent on maintenance once PETRA IV is operational. This contribution presents options for collimator locations, e.g., at the dispersion bump in the achromat cell, to reduce the exposure to losses from the Touschek effect and the injection process. This contribution also quantifies the risk of damaging the installed collimation system in case of hardware failure, e.g., RF cavity or quadrupole failure, since the beam with an emittance of 20 pm could damage collimators if there is no emittance blow-up.

LOSS MECHANISMS IN PETRA IV

The Touschek effect is the major mechanism leading to losses in PETRA IV [1, 2]. Reason for this is the small beam size and large bunch current. Assuming some pessimistic 5% beta-beating along the machine, a beam lifetime of roughly $\tau = 5$ h in the so-called Timing mode (80 high-current bunches with 1 mA bunch current each) and $\tau = 30$ h in the Brightness mode (200 mA distributed on 1600 bunches) is expected. It is therefore crucial to investigate the loss locations of these off-energy particles since the residual-gas scattering lifetime is envisaged to be at least $\tau = 50$ h [3] and is therefore of minor interest. The reduced beam lifetime implies that a power loss in the 170 mW range (Timing mode) will be constantly distributed along the aperture and may cause the demagnetization of permanent magnets within the combined-function dipoles (DLs), undulators and wigglers [4]. It is important to identify locations for potential collimators to intercept these particles before impacting these sensible magnets.

TOUSCHEK-EFFECT LOSSES

Although the dose that determines the risk of inflicting damage onto sensitive hardware has not been estimated yet,

it is important to intercept most Touschek-effect losses to elongate the hardware lifetime substantially in any case.

Potential collimator locations

The ESRF-EBS project uses collimators (scrapers) located at the dispersion bump in the achromat cell to intercept off-energy particles [5]. This strategy is also a potential option for PETRA IV. PETRA IV's hybrid six-bend achromat (H6BA) cells feature a peak dispersion of $D_x = 55$ mm and $D_x = 48$ mm at the location of the potential collimator (approximately 20 cm active material). The optics function and the respective collimator location is shown in Fig. 1. It is worth mentioning that only a handful of collimators are required in PETRA IV and these will be placed in the last cell of the octants that feature the damping wigglers with long straight section following the collimators. This way, the collimation does not take place in the arcs featuring the regular undulators, and it is avoided that these are interacting with a potential shower.

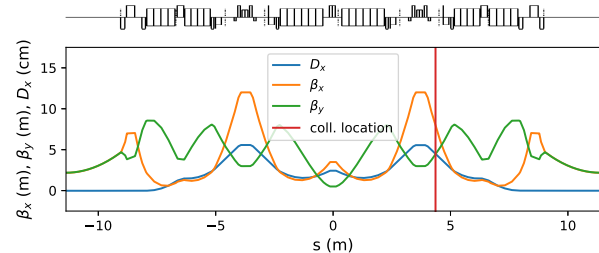


Figure 1: Placement of the collimator within the H6BA cell of PETRA IV. The collimator is located on the falling flank of the dispersion function in the second dispersion bump.

An alternative for collimators in the achromat cells is the introduction of artificial dispersion bumps in the long straight sections for the cost of a larger emittance due to its contributions to the radiation integrals of PETRA IV. Since most of the long straight section feature two ~ 10 m long drifts for accommodating undulators for flagship beam-lines while not all of these slots are occupied, a design idea could be creating the artificial dispersion bumps in multiple of these unoccupied undulators slots. A test has shown that the increase in terms of the emittance for two such of these bumps is in the range of $\Delta\epsilon_x \approx 1.5$ pm for $D_x = 40$ mm in the center of the artificial dispersion bumps. Hence, an increase of $\Delta\epsilon_x \approx 1.5$ pm is already a 7.5% emittance increase. This is the reason this design choice is not envisaged and may only be considered if there is no other effective way of intercepting off-energy particles after the PETRA IV accelerator layout has been finalized.

* marc.andre.jebramcik@desy.de

Simulation of the Touschek effect

In the following, the collimation efficiency of collimators being placed within the H6BA cell is analyzed. PETRA IV features five arcs comprising damping wigglers and three arcs providing synchrotron radiation to beam lines via respective undulators. Hence, collimators could be placed in the last cell of these five arcs. In order to study the effect of the collimator gap as well as the number of collimators, half-gap scans for two, four and ten collimators were performed. The result showed a very weak dependence of the collimation efficiency on the number of collimators. Hence, four collimators that are dedicated to intercept losses from the Touschek effect are envisaged at this point in time. These horizontal collimators will also be able to intercept particles that are injected with a large horizontal action J_x (see next section). The Touschek effect simulation is carried out via the built-in functionality of Elegant [6]. Elegant follows a Monte-Carlo approach for tracking these particles. In order to save computation time, only particles outside the local momentum acceptance (roughly at $\pm 4\%$ energy deviation for PETRA IV) are tracked through the machine. The half-gap scan with four collimators is displayed in Fig. 2. The overall collimation efficiency is slightly lackluster and is potentially insufficient as only approximately 65 % of all Touschek-effect losses are intercepted for acceptable collimator gaps. More than 30 % of the losses get lost at non-critical locations; however, this feature has to be considered with caution since the aperture model may still change slightly. The concept of artificial dispersion bumps in the machine to achieve better collimation could be revisited in the future.

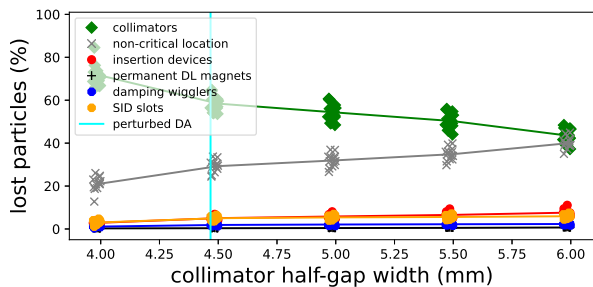


Figure 2: Distribution of losses caused by the Touschek effect in dependence on the half-gap width of the horizontal collimators at the dispersion bump in four H6BA cells.

INJECTION LOSSES

The regularly appearing offsets of the injected beam in terms of its six-dimensional properties has not been studied in detail yet; however, a collimation system that intercepts large transverse and longitudinal actions can be studied now and estimates for the offsets at a later stage can then be embedded into this study. For this purpose, uniform ellipses in $x-x'$, $y-y'$ and $s-\Delta E/E$ spaces respectively are injected and the location of the loss is determined. Ideally, all particles end up hitting a collimator (hard-edge model assumed)

instead of other locations. The half-gap width for the horizontal collimators that counteract losses from the Touschek effect is set to $\Delta x = \pm 4.5$ mm and coincide with the horizontal acceptance $A_x = 2.19 \mu\text{m}$ that matches the value of the expected DA [7]. The vertical collimators have to shield the in-vacuum undulators. To achieve this, two collimators are installed in the southern straight section with vertical phase advance of $\Delta\phi_y \approx \pi/2$ limiting the vertical acceptance to $A_y = 0.39 \mu\text{m}$. Figure 3 shows the restriction of the transverse acceptance of PETRA IV with inserted collimators. The contribution of all collimators to the overall impedance budget is going to be in the 5 % range.

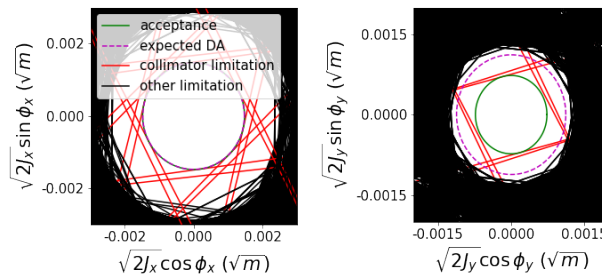


Figure 3: Left: Plot of the aperture limitations projected in the normalized $x-x'$ space with all collimators being inserted. Right: Analogous plot for the $y-y'$ space.

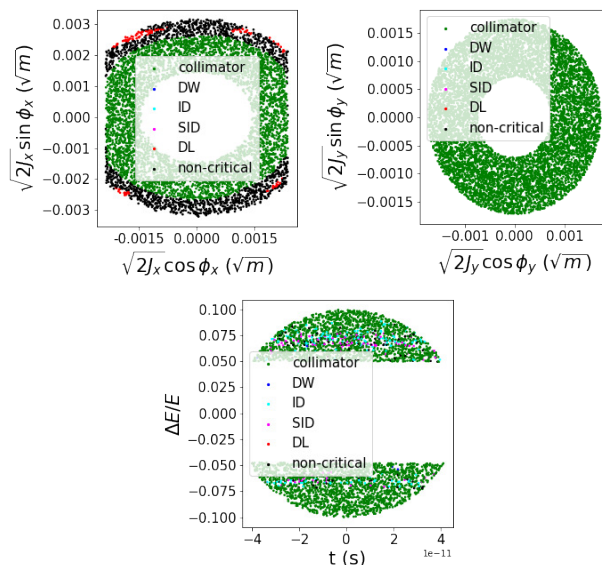


Figure 4: The plots show the initial coordinates of the injected particles with the colors indicating the location of impact on the aperture. While the top left (top right) plot shows the result for a large horizontal (vertical) action J_x (J_y), the bottom plot shows the analogous tracking for a bunch with up to $\Delta E/E = \pm 10\%$ energy offsets.

The loss locations when large ellipses in phase space are injected are shown in Fig. 4. The first two plots show the effectiveness of the collimators to intercept particles just outside the acceptance (green dots). Only for large horizontal

actions in the $J_x > 3.1 \mu\text{m}$ range, particles avoid the collimators and manage to hit damping wigglers (black dots) and DLs (red dots). The misfiring of a single strip-line kicker module [8, 9] that generate the injection bump [10] would cause a central action offset of roughly $\Delta J_x = 0.33 \mu\text{m}$, i.e., the misfiring of a single module is well covered by the collimators. In the absence of the full injection bump, the central action offset of the injected beam is in the $\Delta J_x = 3.5 \mu\text{m}$ range with a pulsed 1-mm thick septum [10]. Particles with such a large action value void the collimators. The bottom plot in Fig. 6 shows the $t-\Delta E/E$ phase space and gives insight regarding the fact why the collimation of Touschek scattered particles is imperfect: While most of the off-energy particles hit the collimators, there is a window in terms of energy offsets roughly centered around $\Delta E/E = \pm 6.5\%$ in which particles impact other parts of the machine like, e.g., undulators, damping wigglers or permanent-magnet dipoles.

COMPONENT FAILURE

In the previous sections, vertical as well as horizontal collimators were inserted into the machine to protect the machine against large transverse actions and particles featuring large energy offsets. Inserting these collimators into PETRA IV with a tiny beam size, however, carries the risk of damaging the collimators (and other devices) if, e.g., the RF voltage fails (RF-OFF scenario) or a quadrupole fails. To determine a potential risk for the aperture, a code that calculates the energy diffusion on the aperture from tracking data is used to determine the maximum energy density per unit mass $(dE/dm)_{\text{max}}$ (dose) on that grid. The functionality of the code is beyond the scope of this contribution; however, it is based on equations given in Ref. [11]. The calculation of the dose is performed for different random seeds for random magnet misalignments. To reduce the energy density on the machine aperture, a kicker that fires once a hardware failure or beam instability is detected can be used to induce filamentation due to amplitude detuning. The dose values with and without such a kicker that induces filamentation is studied for a potential RF-OFF scenario with the previously mentioned horizontal and vertical collimators inserted into the machine. An example evolution of the beam sizes in case a horizontal kicker fires the same moment the RF cavities switch off are shown in Fig. 5. The RF-OFF scenario is of utmost important since slowly reducing the RF voltage may become the desired way of terminating the beam if there is not dedicated extraction [11] (currently tried to be avoided).

RF failure scenario

In the following the RF-OFF scenario is studied with the collimators being inserted. The study is performed for different machine seeds. To showcase the effectiveness of a horizontal kicker to induce filamentation, the peak dose along the circumference is compared between the plain scenario and the scenario with such a kicker. The RF-OFF scenario is studied with 20 random seeds for transverse magnet offsets. The result is shown in Fig. 6. From the plot can be seen that

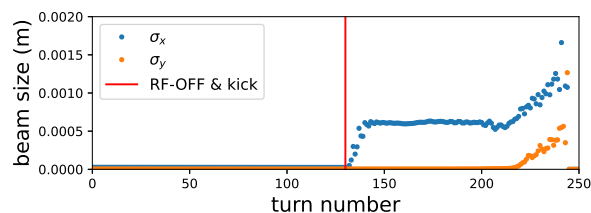


Figure 5: Evolution of the beam size in an error free machine with the RF voltage switching off and the horizontal kicker firing ($\Delta J_x = 8.5 \text{ nm}$ action shift) both in turn number 130.

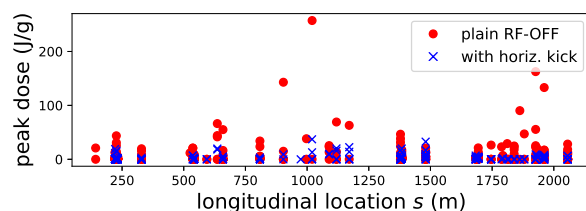


Figure 6: Displayed is the peak dose of 20 error seeds for different transverse misalignments (overlaid) with (blue crosses) and without (red dots) a horizontal kicker that applies a central action shift of $\Delta J_x = 8.5 \text{ nm}$.

a rather large peak dose $(dE/dm)_{\text{max}} > 100 \text{ J/g}$ is inflicted onto the elements that are close to the beam (collimators, IDs). Noteworthy is the a hit with a peak dose of 260 J/g onto a SID slot. This behaviour is highly worrisome; however, Fig. 6 also shows that a applying a horizontal kick the moment the RF fails heavily reduces the peak dose with a maximum among all 20 error seeds of 36 J/g . Such a value could be small enough if such a scenario rarely occurs. A stronger kick can be even more effective as long as it does not immediately lead to stripping particles along the physical aperture. The effectiveness of a kicker to reduce the peak dose in case of a quadrupole fails requires further research as the dose heavily depends on the quadrupole polarity, speed of the field reduction and kicker strength and direction. The ESRF-EBS project [12] features a back-up system to avoid a beam loss in case of a quadrupole failure. The usage of such a system at PETRA IV has also to be analyzed in the future.

CONCLUSION

Collimators within the H6BA cells intercept Touschek-effect particles with an efficiency up to the 65 % range. If the performance is insufficient, other strategies to protect the machine against Touschek-effect losses may have to be revisited. Additional vertical collimators are required to protect the in-vacuum undulators from particles with large vertical action during the injection process. A kicker that causes the blow-up of the beam size seems to mitigate high peak doses in the RF-OFF scenario. An emergency dump systems does not seem necessary at this point in time; however, the quadrupole-failure scenario has not been fully studied and understood yet. Until this point, detailed radiation-shielding simulations have not yet been carried out.

REFERENCES

- [1] C. Schroer *et al.*, “PETRA IV: Upgrade of PETRA III to the Ultimate 3D X-ray Microscope - Conceptual Design Report (CDR)”, DESY, Hamburg, Germany, 2019. doi:10.3204/PUBDB-2019-03613
- [2] I. V. Agapov *et al.*, “PETRA IV Storage Ring Design”, presented at the IPAC’22, Bangkok, Thailand, Jun. 2022, paper TUPOMS014, this conference.
- [3] L. Lilje, private communication, 2022.
- [4] X. M. Maréchal, and T. Shintake, “Radiation damages on permanent magnets: challenges for the future light sources”, in *AIP Conference Proceedings*, vol. 705, no. 282, pp. 282-287, June 2004. doi:10.1063/1.1757789
- [5] R. Versteegen *et al.*, “Collimation scheme for the ESRF Upgrade”, in *Proc. IPAC’15*, Richmond, VA, USA, May 2015, pp. 1434–1437. doi:10.18429/JACoW-IPAC2015-TUPWA017
- [6] M. Borland, “elegant: A Flexible SDDS-Compliant Code for Accelerator Simulation”, Argonne National Laboratory, Lemont, USA, Rep. LS-287, Sep. 2000.
- [7] T. Hellert *et al.*, “Error Analysis and Commissioning Simulation for the PETRA-IV Storage Ring”, presented at the IPAC’22, Bangkok, Thailand, Jun. 2022, paper THPOPT043, this conference.
- [8] G. Loisch, I. V. Agapov, S. A. Antipov, M. A. Jebramcik, J. Keil, and F. Obier, “Stripline Kickers for Injection Into PETRA IV”, in *Proc. IPAC’21*, Campinas, Brazil, May 2021, pp. 2863–2865. doi:10.18429/JACoW-IPAC2021-WEPAB113
- [9] G. Loisch, V. Belokurov, and F. Obier, “Few-Nanosecond Stripline Kickers for Top-Up Injection into PETRA IV”, presented at the IPAC’22, Bangkok, Thailand, Jun. 2022, paper THPOTK040, this conference.
- [10] M. A. Jebramcik *et al.*, “Injection Design Options for the Low-Emittance PETRA IV Storage Ring”, presented at the IPAC’22, Bangkok, Thailand, Jun. 2022, paper THPOPT043, this conference.
- [11] R. Brinkmann, T. Liang, F. Obier, M. Schmitz, “Sweeper Based Emergency Beam Dump System”, DESY, Hamburg, Germany, p4-WP214-rep-0001, Aug. 2020.
- [12] D. Andrault *et al.*, “ESRF upgrade programme phase II (Orange Book)”, ESRF, Grenoble, France, Rep. ESRF, 2014.